

# Ecosystem size and complexity dictate riverine biodiversity

## Supplementary Information for:

Akira Terui\*      Seoghyun Kim\*      Christine L. Dolph<sup>†</sup>      Taku Kadoya<sup>‡</sup>  
Yusuke Miyazaki<sup>§</sup>

## Contents

|   |           |
|---|-----------|
| <b>Fish community data</b>  | <b>1</b>  |
| Hokkaido, Japan . . . . .   | 1         |
| Midwest, US . . . . .   | 2         |
| <b>Tables</b>   | <b>3</b>  |
| Table S1 List of fish species in Hokkaido, Japan . . . . .  | 3         |
| Table S2 List of fish species in Midwest, US . . . . .  | 5         |
| <b>Figures</b>  | <b>9</b>  |
| Figure S1 Influence of ecosystem size ( $p_d = 0.1, \sigma_h = 1, \sigma_l = 0.01$ ) . . . . .            | 9         |
| Figure S2 Influence of ecosystem size ( $p_d = 0.1, \sigma_h = 1, \sigma_l = 1$ ) . . . . .               | 10        |
| Figure S3 Influence of ecosystem size ( $p_d = 0.1, \sigma_h = 0.01, \sigma_l = 0.01$ ) . . . . .         | 11        |
| Figure S4 Influence of ecosystem size ( $p_d = 0.1, \sigma_h = 0.01, \sigma_l = 1$ ) . . . . .            | 12        |
| Figure S5 Influence of ecosystem size ( $p_d = 0.01, \sigma_h = 1, \sigma_l = 1$ ) . . . . .              | 13        |
| Figure S6 Influence of ecosystem size ( $p_d = 0.01, \sigma_h = 0.01, \sigma_l = 0.01$ ) . . . . .        | 14        |
| Figure S7 Influence of ecosystem size ( $p_d = 0.01, \sigma_h = 0.01, \sigma_l = 1$ ) . . . . .           | 15        |
| Figure S8 Influence of ecosystem complexity ( $p_d = 0.1, \sigma_h = 1, \sigma_l = 0.01$ ) . . . . .      | 16        |
| Figure S9 Influence of ecosystem complexity ( $p_d = 0.1, \sigma_h = 1, \sigma_l = 1$ ) . . . . .         | 17        |
| Figure S10 Influence of ecosystem complexity ( $p_d = 0.1, \sigma_h = 0.01, \sigma_l = 0.01$ ) . . . . .  | 18        |
| Figure S11 Influence of ecosystem complexity ( $p_d = 0.1, \sigma_h = 0.01, \sigma_l = 1$ ) . . . . .     | 19        |
| Figure S12 Influence of ecosystem complexity ( $p_d = 0.01, \sigma_h = 1, \sigma_l = 1$ ) . . . . .       | 20        |
| Figure S13 Influence of ecosystem complexity ( $p_d = 0.01, \sigma_h = 0.01, \sigma_l = 0.01$ ) . . . . . | 21        |
| Figure S14 Influence of ecosystem complexity ( $p_d = 0.01, \sigma_h = 0.01, \sigma_l = 1$ ) . . . . .    | 22        |
| <b>References</b>   | <b>23</b> |

## Fish community data

### Hokkaido, Japan

We used data from the Hokkaido Freshwater Fish Database HFish<sup>1</sup>, monitoring data at protected watersheds<sup>2,3</sup>, and primary data collected from literature<sup>4</sup>, which collectively cover the entire Hokkaido island. Data were collected from summer to fall. We screened data through the following procedure:

\*Department of Biology, University of North Carolina at Greensboro

<sup>†</sup>Department of Ecology, Evolution and Behavior, University of Minnesota

<sup>‡</sup>National Institute for Environmental Studies

<sup>§</sup>Shiraume Gakuen University

1. We listed recorded fish species and re-organized species names to be consistent across the data sets.
2. We selected sampling sites based on the following criteria: (1) surveys were conducted with netting and/or electrofishing, (2) surveys were designed to collect a whole fish community, (3) sites contained reliable coordinates (sites with coordinates identical at 3 decimal degrees were treated as the same site), and (4) sites did not involve unidentified species that are rarely observed in the data set ( $< 100$  sites occurrence).
3. For sites with multiple visits (i.e., temporal replicates), we used the latest-year observation at each sampling site to minimize variation in sampling efforts among sites. Surveys that occurred in the same year were aggregated into a single observation.
4. We confined sites to those with the latest observation year of  $\geq 1990$ . Although the data set contained observations from 1953, we added this restriction to align the observation period with the data set in the Midwest, US.
5. Four genera (Lethenteron, Pungitius, Rhinogobius, and Tribolodon) were treated as species groups (i.e., spp.) as taxonomic resolutions varied greatly among data sources.

## Midwest, US

We assembled fish community data collected by the Iowa Department of Natural Resources, Illinois Environmental Protection Agency and Illinois Department of Natural Resources, Minnesota Pollution Control Agency, and Wisconsin Department of Natural Resources. These data sets cover most of Upper Mississippi (HUC 2, region 07) and the part of Great Lakes (HUC 2, region 04), Missouri (HUC 2, region 10), and Ohio (HUC 2, region 05). Data were collected from summer to fall with electrofishing (backpack, barge-type, or boat-mounted) and supplemental netting at some locations. We screened data through the following procedure:

1. We used data of the Upper Mississippi (HUC 2, region 07) and Great Lakes basins (HUC 2, region 04) as most sites are included in these regions.
2. We removed records of unidentified species, hybrid species, and commercial species that are apparently absent in the wild (e.g., goldfish).
3. We used the latest observation at each sampling site to minimize variation in sampling efforts among sites.

## Tables

**Table S1 List of fish species in Hokkaido, Japan**

List of fish species in Hokkaido, Japan that are included in our statistical analysis. 52 species are ordered alphabetically with the number of sites present and % occupancy out of 2592 sites.

| Species                                   | Number of sites present | Occupancy (%) |
|---|-------------------------|---------------|
| <i>Acanthogobius lactipes</i>             | 63                      | 2.43          |
| <i>Anguilla japonica</i>                  | 1                       | 0.04          |
| <i>Carassius buergeri</i> subsp. 2        | 4                       | 0.15          |
| <i>Carassius cuvieri</i>                  | 24                      | 0.93          |
| <i>Carassius</i> sp.                      | 213                     | 8.22          |
| <i>Channa argus</i>                       | 3                       | 0.12          |
| <i>Cottus amblystomopsis</i>              | 48                      | 1.85          |
| <i>Cottus hangiongensis</i>               | 94                      | 3.63          |
| <i>Cottus nozawae</i>                     | 833                     | 32.14         |
| <i>Cottus</i> sp. ME                      | 25                      | 0.96          |
| <i>Cyprinus carpio</i>                    | 50                      | 1.93          |
| <i>Gasterosteus aculeatus</i>             | 147                     | 5.67          |
| <i>Gnathopogon caeruleus</i>              | 1                       | 0.04          |
| <i>Gnathopogon elongatus elongatus</i>    | 2                       | 0.08          |
| <i>Gymnogobius breunigii</i>              | 29                      | 1.12          |
| <i>Gymnogobius castaneus</i> complex      | 145                     | 5.59          |
| <i>Gymnogobius opperiens</i>              | 85                      | 3.28          |
| <i>Gymnogobius petschiliensis</i>         | 2                       | 0.08          |
| <i>Gymnogobius urotaenia</i>              | 290                     | 11.19         |
| <i>Hucho perryi</i>                       | 61                      | 2.35          |
| <i>Hypomesus nipponensis</i>              | 170                     | 6.56          |
| <i>Hypomesus olidus</i>                   | 8                       | 0.31          |
| <i>Lefua nikkonis</i>                     | 20                      | 0.77          |
| <i>Lethenteron</i> spp.                   | 731                     | 28.20         |
| <i>Leucopsarion petersii</i>              | 3                       | 0.12          |
| <i>Luciogobius guttatus</i>               | 3                       | 0.12          |
| <i>Misgurnus anguillicaudatus</i>         | 212                     | 8.18          |
| <i>Noemacheilus barbatulus</i>            | 1590                    | 61.34         |
| <i>Oncorhynchus gorbuscha</i>             | 27                      | 1.04          |
| <i>Oncorhynchus keta</i>                  | 150                     | 5.79          |
| <i>Oncorhynchus masou masou</i>           | 1417                    | 54.67         |
| <i>Oncorhynchus mykiss</i>                | 462                     | 17.82         |
| <i>Oncorhynchus nerka</i>                 | 6                       | 0.23          |
| <i>Opsariichthys platypus</i>             | 1                       | 0.04          |
| <i>Osmerus dentex</i>                     | 7                       | 0.27          |
| <i>Phoxinus phoxinus sachalinensis</i>    | 68                      | 2.62          |
| <i>Plecoglossus altivelis altivelis</i>   | 111                     | 4.28          |
| <i>Pseudorasbora parva</i>                | 94                      | 3.63          |
| <i>Pungitius</i> spp.                     | 285                     | 11.00         |
| <i>Rhinogobius</i> spp.                   | 175                     | 6.75          |
| <i>Rhodeus ocellatus ocellatus</i>        | 22                      | 0.85          |
| <i>Salangichthys microdon</i>             | 11                      | 0.42          |
| <i>Salmo trutta</i>                       | 15                      | 0.58          |
| <i>Salvelinus fontinalis</i>              | 2                       | 0.08          |
| <i>Salvelinus leucomaenis leucomaenis</i> | 625                     | 24.11         |
| <i>Salvelinus malma</i>                   | 274                     | 10.57         |

| Species                  | Number of sites present | Occupancy (%) |
|--------------------------|-------------------------|---------------|
| Salvelinus malma miyabei | 2                       | 0.08          |
| Silurus asotus           | 7                       | 0.27          |
| Spirinchus lanceolatus   | 7                       | 0.27          |
| Tribolodon spp.          | 1163                    | 44.87         |
| Tridentiger brevispinis  | 135                     | 5.21          |
| Tridentiger obscurus     | 7                       | 0.27          |

## Table S2 List of fish species in Midwest, US

List of fish species in Midwest, US that are included in our statistical analysis. 159 species are ordered alphabetically with the number of sites present and % occupancy out of 3998 sites.

| Species                             | Number of sites present | Occupancy (%) |
|-------------------------------------|-------------------------|---------------|
| <i>Acipenser fulvescens</i>         | 7                       | 0.18          |
| <i>Alosa pseudoharengus</i>         | 1                       | 0.03          |
| <i>Ambloplites rupestris</i>        | 707                     | 17.68         |
| <i>Ameiurus melas</i>               | 868                     | 21.71         |
| <i>Ameiurus natalis</i>             | 665                     | 16.63         |
| <i>Ameiurus nebulosus</i>           | 30                      | 0.75          |
| <i>Amia calva</i>                   | 95                      | 2.38          |
| <i>Ammocrypta clara</i>             | 12                      | 0.30          |
| <i>Aphredoderus sayanus</i>         | 76                      | 1.90          |
| <i>Aplodinotus grunniens</i>        | 208                     | 5.20          |
| <i>Campostoma anomalum</i>          | 1347                    | 33.69         |
| <i>Campostoma oligolepis</i>        | 125                     | 3.13          |
| <i>Carpionodes carpio</i>           | 128                     | 3.20          |
| <i>Carpionodes cyprinus</i>         | 234                     | 5.85          |
| <i>Carpionodes velifer</i>          | 82                      | 2.05          |
| <i>Catostomus commersonii</i>       | 2931                    | 73.31         |
| <i>Centrarchus macropterus</i>      | 5                       | 0.13          |
| <i>Chrosomus eos</i>                | 336                     | 8.40          |
| <i>Chrosomus neogaeus</i>           | 103                     | 2.58          |
| <i>Clinostomus elongatus</i>        | 97                      | 2.43          |
| <i>Cottus bairdii</i>               | 467                     | 11.68         |
| <i>Cottus carolinae</i>             | 6                       | 0.15          |
| <i>Cottus cognatus</i>              | 38                      | 0.95          |
| <i>Crystallaria asprella</i>        | 1                       | 0.03          |
| <i>Ctenopharyngodon idella</i>      | 19                      | 0.48          |
| <i>Culaea inconstans</i>            | 1531                    | 38.29         |
| <i>Cyprinella lutrensis</i>         | 269                     | 6.73          |
| <i>Cyprinella spiloptera</i>        | 780                     | 19.51         |
| <i>Cyprinella venusta</i>           | 2                       | 0.05          |
| <i>Cyprinella whipplei</i>          | 33                      | 0.83          |
| <i>Cyprinus carpio</i>              | 946                     | 23.66         |
| <i>Dorosoma cepedianum</i>          | 208                     | 5.20          |
| <i>Erimystax x-punctatus</i>        | 13                      | 0.33          |
| <i>Erimyzon oblongus</i>            | 63                      | 1.58          |
| <i>Erimyzon sucetta</i>             | 10                      | 0.25          |
| <i>Esox americanus vermiculatus</i> | 117                     | 2.93          |
| <i>Esox lucius</i>                  | 957                     | 23.94         |
| <i>Esox masquinongy</i>             | 20                      | 0.50          |
| <i>Etheostoma asprigene</i>         | 10                      | 0.25          |
| <i>Etheostoma blennioides</i>       | 1                       | 0.03          |
| <i>Etheostoma caeruleum</i>         | 195                     | 4.88          |
| <i>Etheostoma chlorosomum</i>       | 4                       | 0.10          |
| <i>Etheostoma crossopterus</i>      | 4                       | 0.10          |
| <i>Etheostoma exile</i>             | 261                     | 6.53          |
| <i>Etheostoma flabellare</i>        | 843                     | 21.09         |
| <i>Etheostoma gracile</i>           | 15                      | 0.38          |
| <i>Etheostoma kennicotti</i>        | 1                       | 0.03          |
| <i>Etheostoma microperca</i>        | 20                      | 0.50          |

| Species                            | Number of sites present | Occupancy (%) |
|------------------------------------|-------------------------|---------------|
| <i>Etheostoma nigrum</i>           | 2546                    | 63.68         |
| <i>Etheostoma proeliare</i>        | 2                       | 0.05          |
| <i>Etheostoma spectabile</i>       | 121                     | 3.03          |
| <i>Etheostoma squamiceps</i>       | 4                       | 0.10          |
| <i>Etheostoma zonale</i>           | 321                     | 8.03          |
| <i>Fundulus diaphanus</i>          | 3                       | 0.08          |
| <i>Fundulus dispar</i>             | 4                       | 0.10          |
| <i>Fundulus notatus</i>            | 282                     | 7.05          |
| <i>Fundulus olivaceus</i>          | 42                      | 1.05          |
| <i>Hiodon alosoides</i>            | 3                       | 0.08          |
| <i>Hiodon tergisus</i>             | 16                      | 0.40          |
| <i>Hybognathus hankinsoni</i>      | 576                     | 14.41         |
| <i>Hybognathus nuchalis</i>        | 24                      | 0.60          |
| <i>Hybopsis amnis</i>              | 1                       | 0.03          |
| <i>Hypentelium nigricans</i>       | 682                     | 17.06         |
| <i>Hypophthalmichthys molitrix</i> | 14                      | 0.35          |
| <i>Hypophthalmichthys nobilis</i>  | 3                       | 0.08          |
| <i>Ichthyomyzon castaneus</i>      | 51                      | 1.28          |
| <i>Ichthyomyzon fossor</i>         | 35                      | 0.88          |
| <i>Ichthyomyzon gagei</i>          | 6                       | 0.15          |
| <i>Ichthyomyzon unicuspis</i>      | 9                       | 0.23          |
| <i>Ictalurus punctatus</i>         | 413                     | 10.33         |
| <i>Ictiobus bubalus</i>            | 90                      | 2.25          |
| <i>Ictiobus cyprinellus</i>        | 129                     | 3.23          |
| <i>Ictiobus niger</i>              | 41                      | 1.03          |
| <i>Labidesthes sicculus</i>        | 64                      | 1.60          |
| <i>Lepisosteus oculatus</i>        | 13                      | 0.33          |
| <i>Lepisosteus osseus</i>          | 25                      | 0.63          |
| <i>Lepisosteus platostomus</i>     | 58                      | 1.45          |
| <i>Lepomis cyanellus</i>           | 1575                    | 39.39         |
| <i>Lepomis gibbosus</i>            | 290                     | 7.25          |
| <i>Lepomis gulosus</i>             | 43                      | 1.08          |
| <i>Lepomis humilis</i>             | 356                     | 8.90          |
| <i>Lepomis macrochirus</i>         | 1051                    | 26.29         |
| <i>Lepomis megalotis</i>           | 186                     | 4.65          |
| <i>Lepomis microlophus</i>         | 19                      | 0.48          |
| <i>Lethenteron appendix</i>        | 122                     | 3.05          |
| <i>Lota lota</i>                   | 266                     | 6.65          |
| <i>Luxilus chrysocephalus</i>      | 198                     | 4.95          |
| <i>Luxilus cornutus</i>            | 1784                    | 44.62         |
| <i>Lythrurus fumeus</i>            | 6                       | 0.15          |
| <i>Lythrurus umbratilis</i>        | 224                     | 5.60          |
| <i>Macrhybopsis aestivalis</i>     | 1                       | 0.03          |
| <i>Macrhybopsis hyostoma</i>       | 3                       | 0.08          |
| <i>Macrhybopsis storeriana</i>     | 10                      | 0.25          |
| <i>Micropterus dolomieu</i>        | 748                     | 18.71         |
| <i>Micropterus punctulatus</i>     | 15                      | 0.38          |
| <i>Micropterus salmoides</i>       | 987                     | 24.69         |
| <i>Minytrema melanops</i>          | 41                      | 1.03          |
| <i>Morone americana</i>            | 2                       | 0.05          |
| <i>Morone chrysops</i>             | 65                      | 1.63          |
| <i>Morone mississippiensis</i>     | 16                      | 0.40          |

| Species                        | Number of sites present | Occupancy (%) |
|--------------------------------|-------------------------|---------------|
| Moxostoma anisurum             | 288                     | 7.20          |
| Moxostoma carinatum            | 8                       | 0.20          |
| Moxostoma duquesni             | 103                     | 2.58          |
| Moxostoma erythrurum           | 709                     | 17.73         |
| Moxostoma macrolepidotum       | 737                     | 18.43         |
| Moxostoma valenciennesi        | 85                      | 2.13          |
| Neogobius melanostomus         | 13                      | 0.33          |
| Nocomis biguttatus             | 1287                    | 32.19         |
| Notemigonus crysoleucas        | 377                     | 9.43          |
| Notropis anogenus              | 10                      | 0.25          |
| Notropis atherinoides          | 207                     | 5.18          |
| Notropis blennius              | 16                      | 0.40          |
| Notropis boops                 | 9                       | 0.23          |
| Notropis buccatus              | 47                      | 1.18          |
| Notropis chalybaeus            | 11                      | 0.28          |
| Notropis dorsalis              | 1088                    | 27.21         |
| Notropis heterodon             | 28                      | 0.70          |
| Notropis heterolepis           | 187                     | 4.68          |
| Notropis hudsonius             | 81                      | 2.03          |
| Notropis nubilus               | 58                      | 1.45          |
| Notropis percobromus           | 167                     | 4.18          |
| Notropis rubellus              | 63                      | 1.58          |
| Notropis stramineus            | 975                     | 24.39         |
| Notropis texanus               | 20                      | 0.50          |
| Notropis volucellus            | 81                      | 2.03          |
| Notropis wickliffi             | 10                      | 0.25          |
| Noturus exilis                 | 34                      | 0.85          |
| Noturus flavus                 | 479                     | 11.98         |
| Noturus gyrinus                | 447                     | 11.18         |
| Noturus nocturnus              | 38                      | 0.95          |
| Oncorhynchus mykiss            | 55                      | 1.38          |
| Oncorhynchus tshawytscha       | 1                       | 0.03          |
| Opsopoeodus emiliae            | 3                       | 0.08          |
| Perca flavescens               | 622                     | 15.56         |
| Percina caprodes               | 337                     | 8.43          |
| Percina carprodes semifasciata | 7                       | 0.18          |
| Percina evides                 | 16                      | 0.40          |
| Percina maculata               | 888                     | 22.21         |
| Percina phoxocephala           | 259                     | 6.48          |
| Percina sciera                 | 2                       | 0.05          |
| Percopsis omiscomaycus         | 21                      | 0.53          |
| Phenacobius mirabilis          | 259                     | 6.48          |
| Phoxinus erythrogaster         | 417                     | 10.43         |
| Pimephales notatus             | 1784                    | 44.62         |
| Pimephales promelas            | 1535                    | 38.39         |
| Pimephales vigilax             | 84                      | 2.10          |
| Pomoxis annularis              | 61                      | 1.53          |
| Pomoxis nigromaculatus         | 376                     | 9.40          |
| Pylodictis olivaris            | 73                      | 1.83          |
| Rhinichthys atratulus          | 1120                    | 28.01         |
| Rhinichthys cataractae         | 627                     | 15.68         |
| Rhinichthys obtusus            | 449                     | 11.23         |

| Species                             | Number of sites present | Occupancy (%) |
|-------------------------------------|-------------------------|---------------|
| <i>Salmo trutta</i>                 | 399                     | 9.98          |
| <i>Salvelinus fontinalis</i>        | 369                     | 9.23          |
| <i>Sander canadensis</i>            | 39                      | 0.98          |
| <i>Sander vitreus</i>               | 367                     | 9.18          |
| <i>Scaphirhynchus platyrhynchus</i> | 8                       | 0.20          |
| <i>Semotilus atromaculatus</i>      | 2776                    | 69.43         |
| <i>Umbra limi</i>                   | 1600                    | 40.02         |



## Figures

**Figure S1 Influence of ecosystem size ( $p_d = 0.1$ ,  $\sigma_h = 1$ ,  $\sigma_l = 0.01$ )**

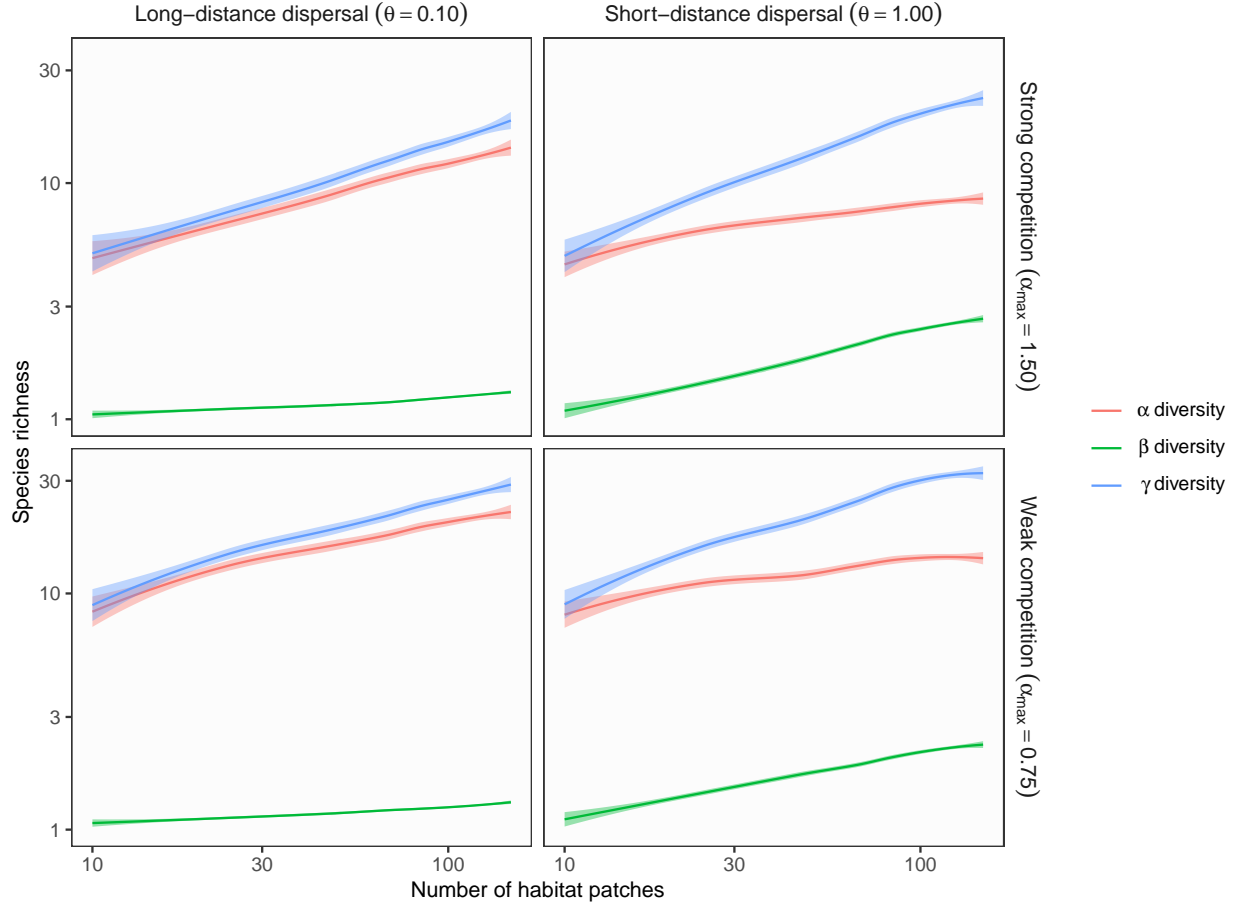


**Figure S1** Theoretical predictions for ecosystem size influences (the number of habitat patches) on  $\alpha$ ,  $\beta$ , and  $\gamma$  diversity in branching networks. In this simulation, environmental variation at headwaters ( $\sigma_h$ ) exceeds local environmental noise ( $\sigma_l$ ). Lines and shades are loess curves fitted to simulated data and its 95% confidence intervals. Each panel represents different ecological scenarios under which metacommunity dynamics were simulated. Rows represent different competition strength. Competitive coefficients ( $\alpha_{ij}$ ) were varied randomly from 0 to 1.5 (top, strong competition) or 0.75 (bottom, weak competition). Columns represent different dispersal scenarios. Two dispersal parameters were chosen to simulate scenarios with long-distance (the rate parameter of an exponential dispersal kernel  $\theta = 0.10$ ) and short-distance dispersal ( $\theta = 1.0$ ). Other parameters are as follows: dispersal probability  $p_d = 0.1$ ; environmental variation at headwaters  $\sigma_h = 1$ ; local environmental noise  $\sigma_l = 0.01$ .

**Figure S2 Influence of ecosystem size ( $p_d = 0.1$ ,  $\sigma_h = 1$ ,  $\sigma_l = 1$ )**

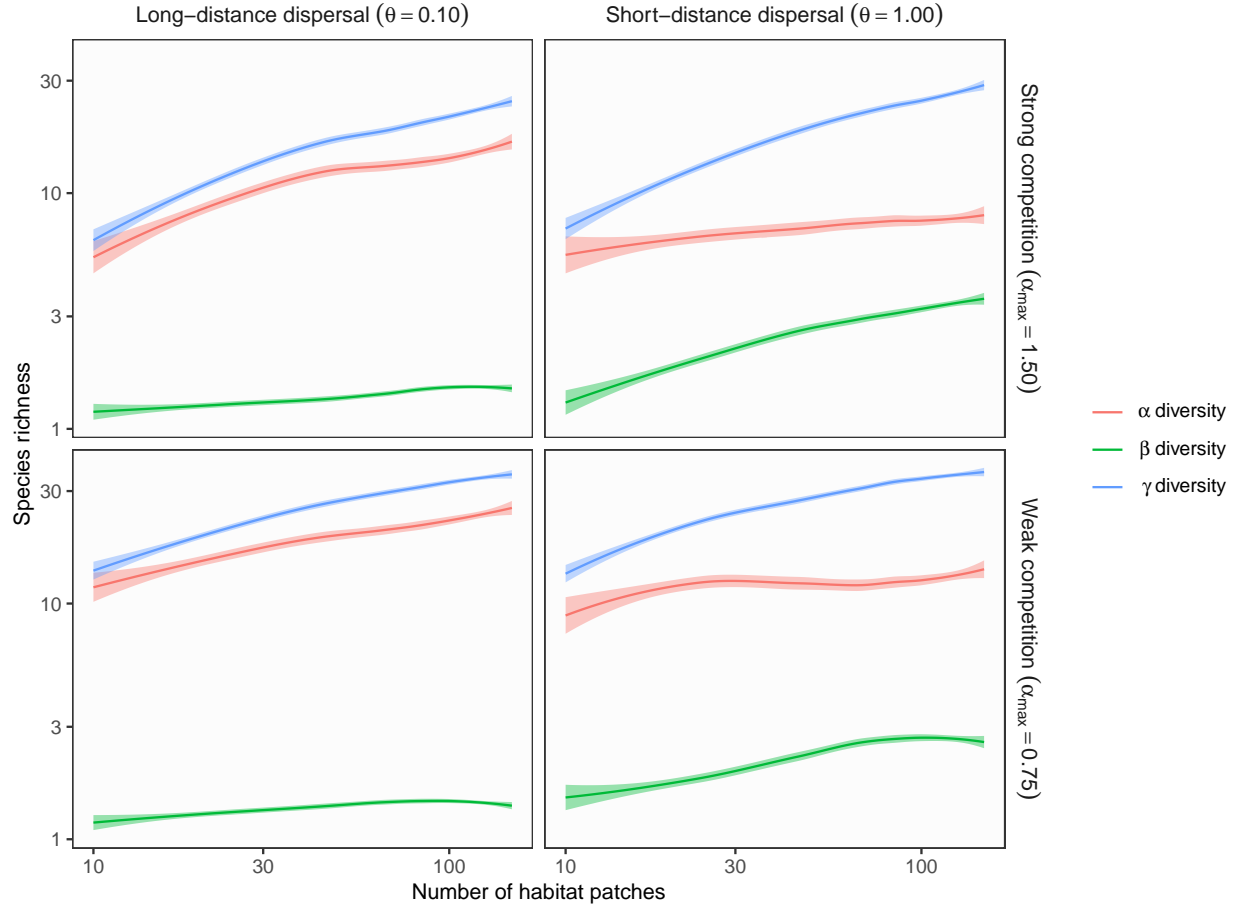


**Figure S2** Theoretical predictions for ecosystem size influences (the number of habitat patches) on  $\alpha$ ,  $\beta$ , and  $\gamma$  diversity in branching networks. In this simulation, environmental variation at headwaters ( $\sigma_h$ ) is equal to local environmental noise ( $\sigma_l$ ). Lines and shades are loess curves fitted to simulated data and its 95% confidence intervals. Each panel represents different ecological scenarios under which metacommunity dynamics were simulated. Rows represent different competition strength. Competitive coefficients ( $\alpha_{ij}$ ) were varied randomly from 0 to 1.5 (top, strong competition) or 0.75 (bottom, weak competition). Columns represent different dispersal scenarios. Two dispersal parameters were chosen to simulate scenarios with long-distance (the rate parameter of an exponential dispersal kernel  $\theta = 0.10$ ) and short-distance dispersal ( $\theta = 1.0$ ). Other parameters are as follows: dispersal probability  $p_d = 0.1$ ; environmental variation at headwaters  $\sigma_h = 1$ ; local environmental noise  $\sigma_l = 1$ .

**Figure S3 Influence of ecosystem size ( $p_d = 0.1$ ,  $\sigma_h = 0.01$ ,  $\sigma_l = 0.01$ )**

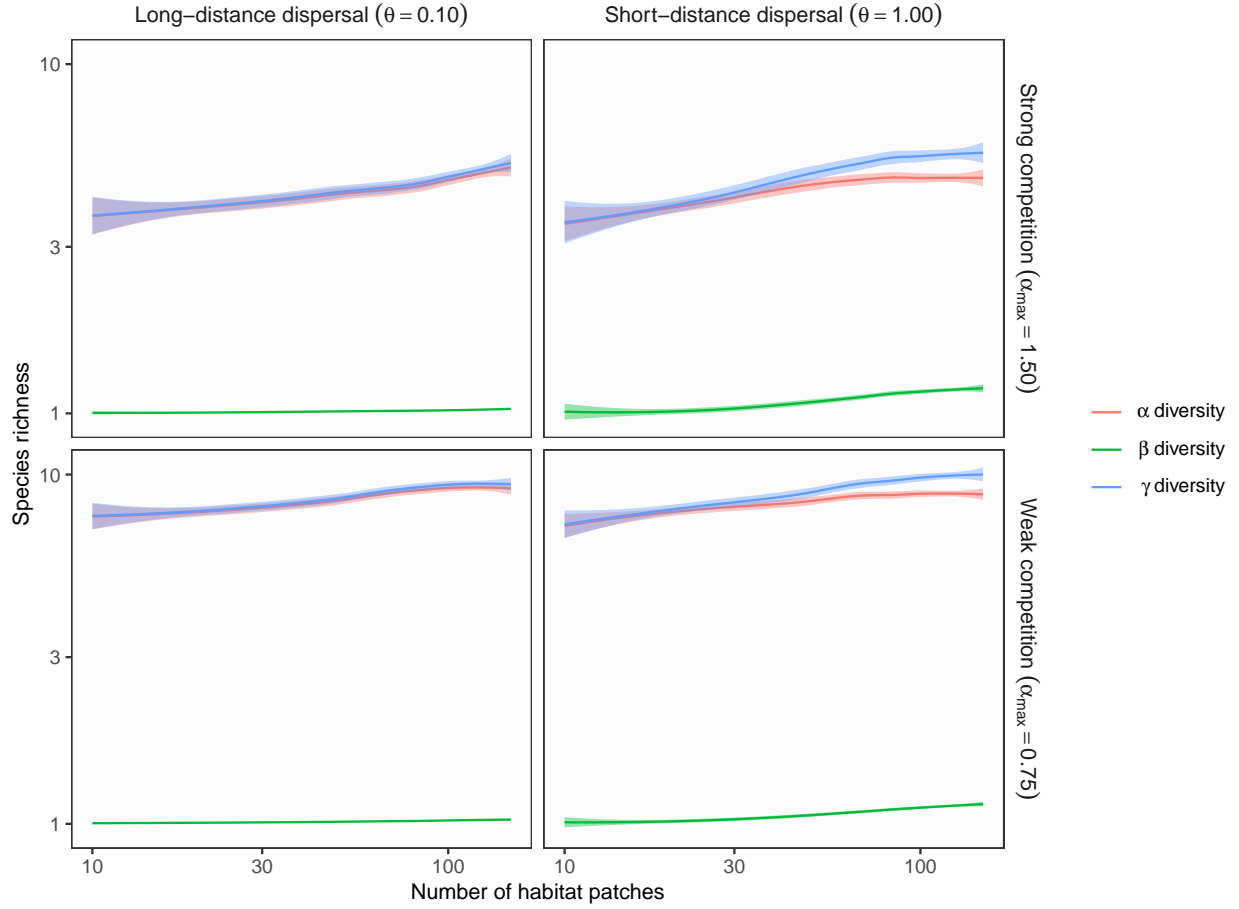


**Figure S3** Theoretical predictions for ecosystem size influences (the number of habitat patches) on  $\alpha$ ,  $\beta$ , and  $\gamma$  diversity in branching networks. In this simulation, environmental variation at headwaters ( $\sigma_h$ ) is equal to local environmental noise ( $\sigma_l$ ). Lines and shades are loess curves fitted to simulated data and its 95% confidence intervals. Each panel represents different ecological scenarios under which metacommunity dynamics were simulated. Rows represent different competition strength. Competitive coefficients ( $\alpha_{ij}$ ) were varied randomly from 0 to 1.5 (top, strong competition) or 0.75 (bottom, weak competition). Columns represent different dispersal scenarios. Two dispersal parameters were chosen to simulate scenarios with long-distance (the rate parameter of an exponential dispersal kernel  $\theta = 0.10$ ) and short-distance dispersal ( $\theta = 1.0$ ). Other parameters are as follows: dispersal probability  $p_d = 0.1$ ; environmental variation at headwaters  $\sigma_h = 0.01$ ; local environmental noise  $\sigma_l = 0.01$ .

**Figure S4 Influence of ecosystem size ( $p_d = 0.1$ ,  $\sigma_h = 0.01$ ,  $\sigma_l = 1$ )**

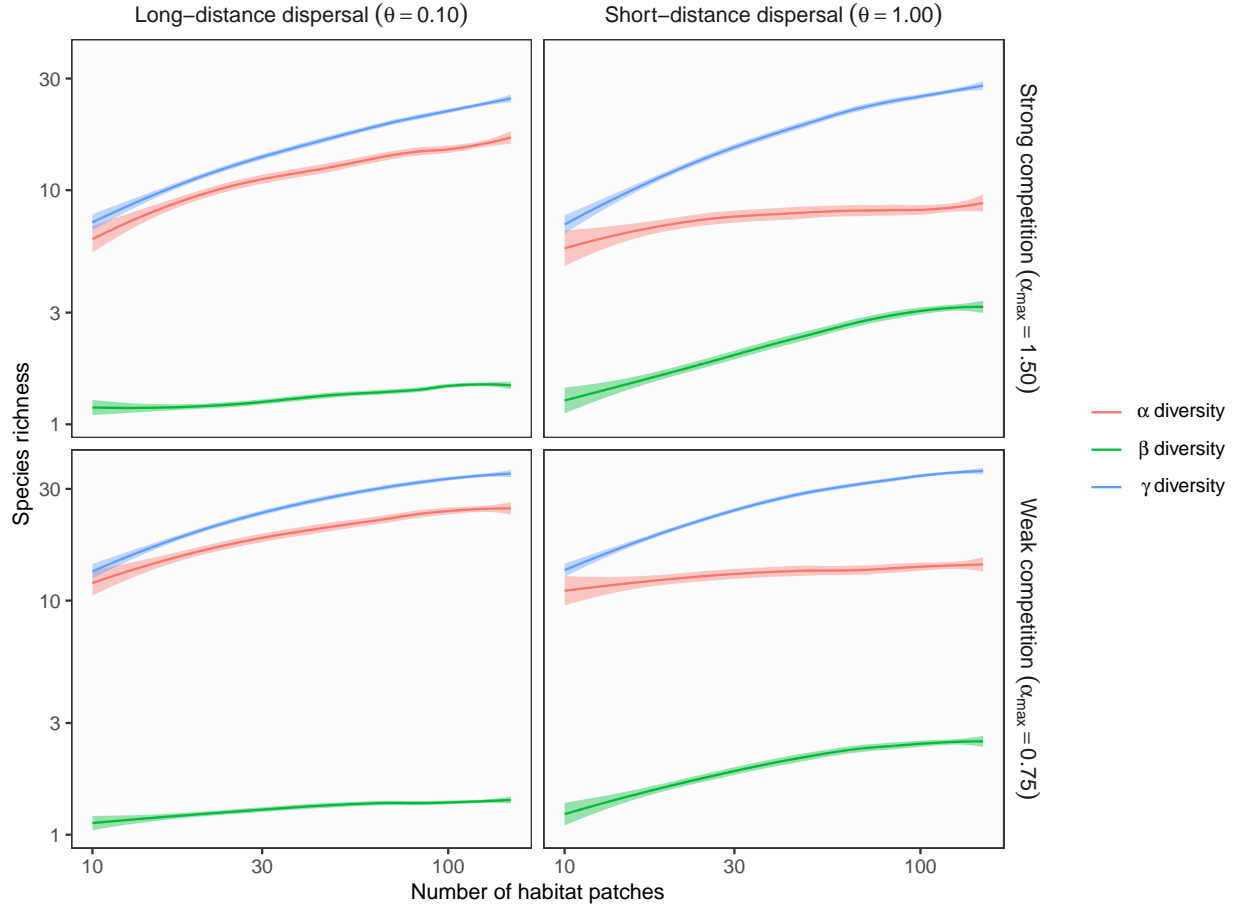


**Figure S4** Theoretical predictions for ecosystem size influences (the number of habitat patches) on  $\alpha$ ,  $\beta$ , and  $\gamma$  diversity in branching networks. In this simulation, environmental variation at headwaters ( $\sigma_h$ ) is less than local environmental noise ( $\sigma_l$ ). Lines and shades are loess curves fitted to simulated data and its 95% confidence intervals. Each panel represents different ecological scenarios under which metacommunity dynamics were simulated. Rows represent different competition strength. Competitive coefficients ( $\alpha_{ij}$ ) were varied randomly from 0 to 1.5 (top, strong competition) or 0.75 (bottom, weak competition). Columns represent different dispersal scenarios. Two dispersal parameters were chosen to simulate scenarios with long-distance (the rate parameter of an exponential dispersal kernel  $\theta = 0.10$ ) and short-distance dispersal ( $\theta = 1.0$ ). Other parameters are as follows: dispersal probability  $p_d = 0.1$ ; environmental variation at headwaters  $\sigma_h = 0.01$ ; local environmental noise  $\sigma_l = 1$ .

**Figure S5 Influence of ecosystem size ( $p_d = 0.01$ ,  $\sigma_h = 1$ ,  $\sigma_l = 1$ )**

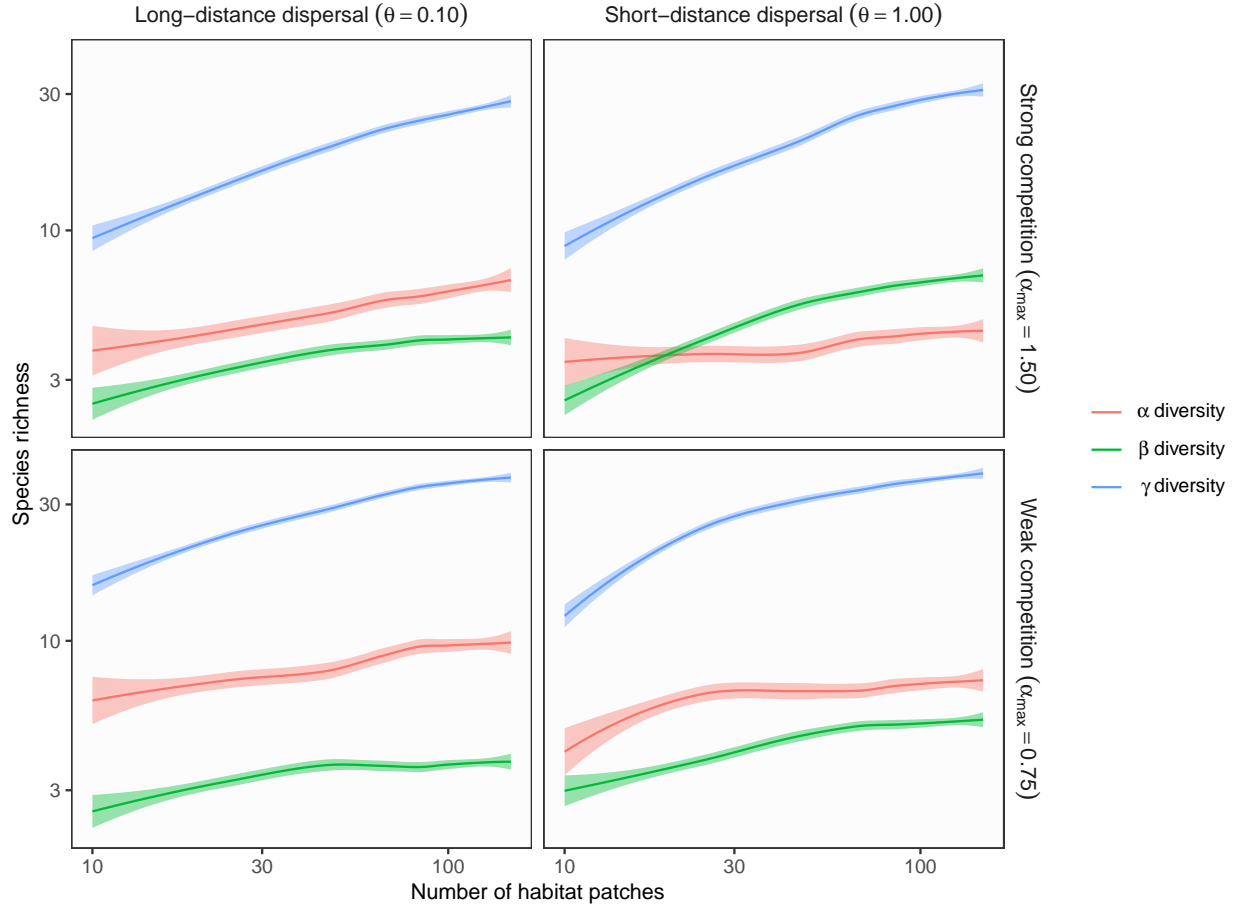


**Figure S5** Theoretical predictions for ecosystem size influences (the number of habitat patches) on  $\alpha$ ,  $\beta$ , and  $\gamma$  diversity in branching networks. In this simulation, environmental variation at headwaters ( $\sigma_h$ ) is equal to local environmental noise ( $\sigma_l$ ). Lines and shades are loess curves fitted to simulated data and its 95% confidence intervals. Each panel represents different ecological scenarios under which metacommunity dynamics were simulated. Rows represent different competition strength. Competitive coefficients ( $\alpha_{ij}$ ) were varied randomly from 0 to 1.5 (top, strong competition) or 0.75 (bottom, weak competition). Columns represent different dispersal scenarios. Two dispersal parameters were chosen to simulate scenarios with long-distance (the rate parameter of an exponential dispersal kernel  $\theta = 0.10$ ) and short-distance dispersal ( $\theta = 1.0$ ). Other parameters are as follows: dispersal probability  $p_d = 0.01$ ; environmental variation at headwaters  $\sigma_h = 1$ ; local environmental noise  $\sigma_l = 1$ .

**Figure S6 Influence of ecosystem size ( $p_d = 0.01$ ,  $\sigma_h = 0.01$ ,  $\sigma_l = 0.01$ )**

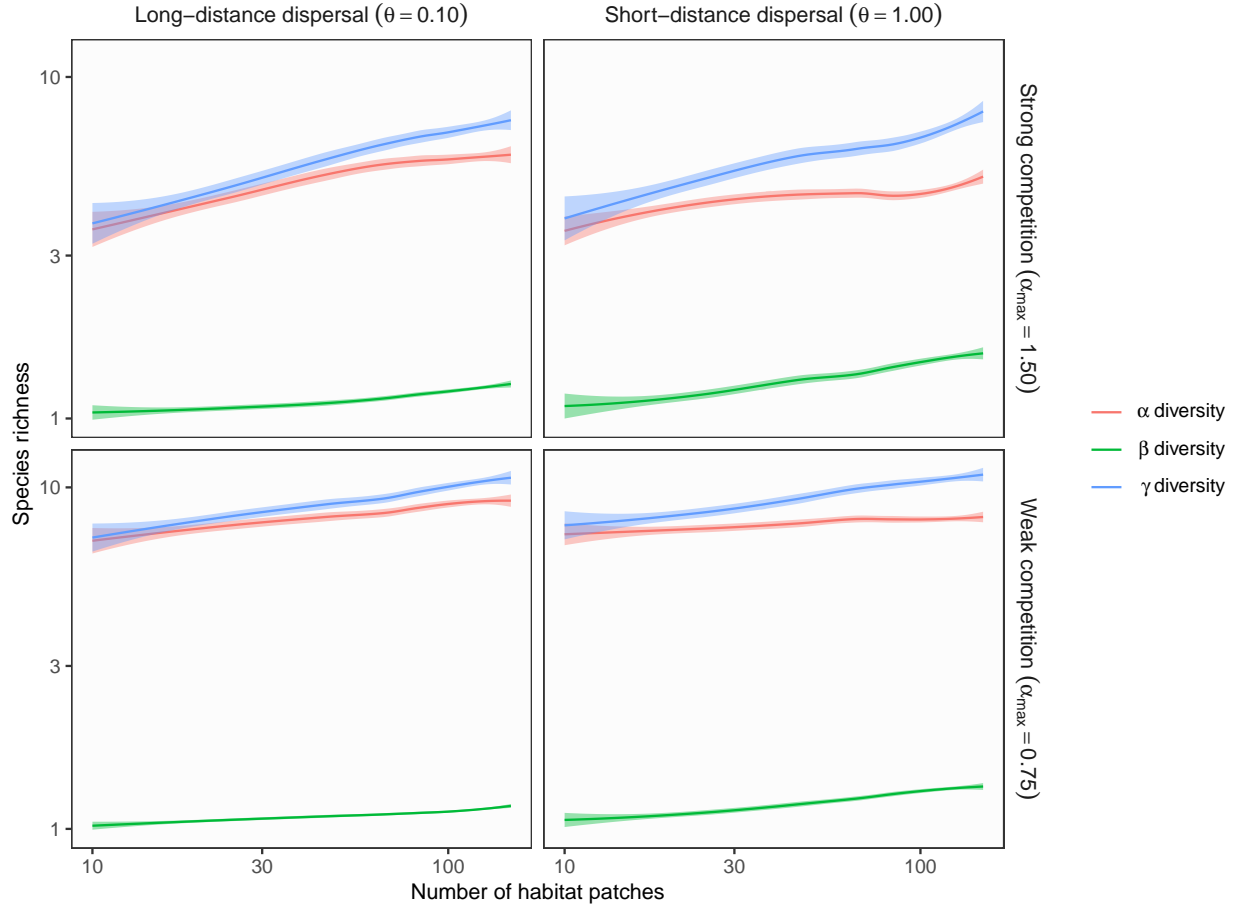


**Figure S6** Theoretical predictions for ecosystem size influences (the number of habitat patches) on  $\alpha$ ,  $\beta$ , and  $\gamma$  diversity in branching networks. In this simulation, environmental variation at headwaters ( $\sigma_h$ ) is equal to local environmental noise ( $\sigma_l$ ). Lines and shades are loess curves fitted to simulated data and its 95% confidence intervals. Each panel represents different ecological scenarios under which metacommunity dynamics were simulated. Rows represent different competition strength. Competitive coefficients ( $\alpha_{ij}$ ) were varied randomly from 0 to 1.5 (top, strong competition) or 0.75 (bottom, weak competition). Columns represent different dispersal scenarios. Two dispersal parameters were chosen to simulate scenarios with long-distance (the rate parameter of an exponential dispersal kernel  $\theta = 0.10$ ) and short-distance dispersal ( $\theta = 1.0$ ). Other parameters are as follows: dispersal probability  $p_d = 0.01$ ; environmental variation at headwaters  $\sigma_h = 0.01$ ; local environmental noise  $\sigma_l = 0.01$ .

**Figure S7 Influence of ecosystem size ( $p_d = 0.01$ ,  $\sigma_h = 0.01$ ,  $\sigma_l = 1$ )**

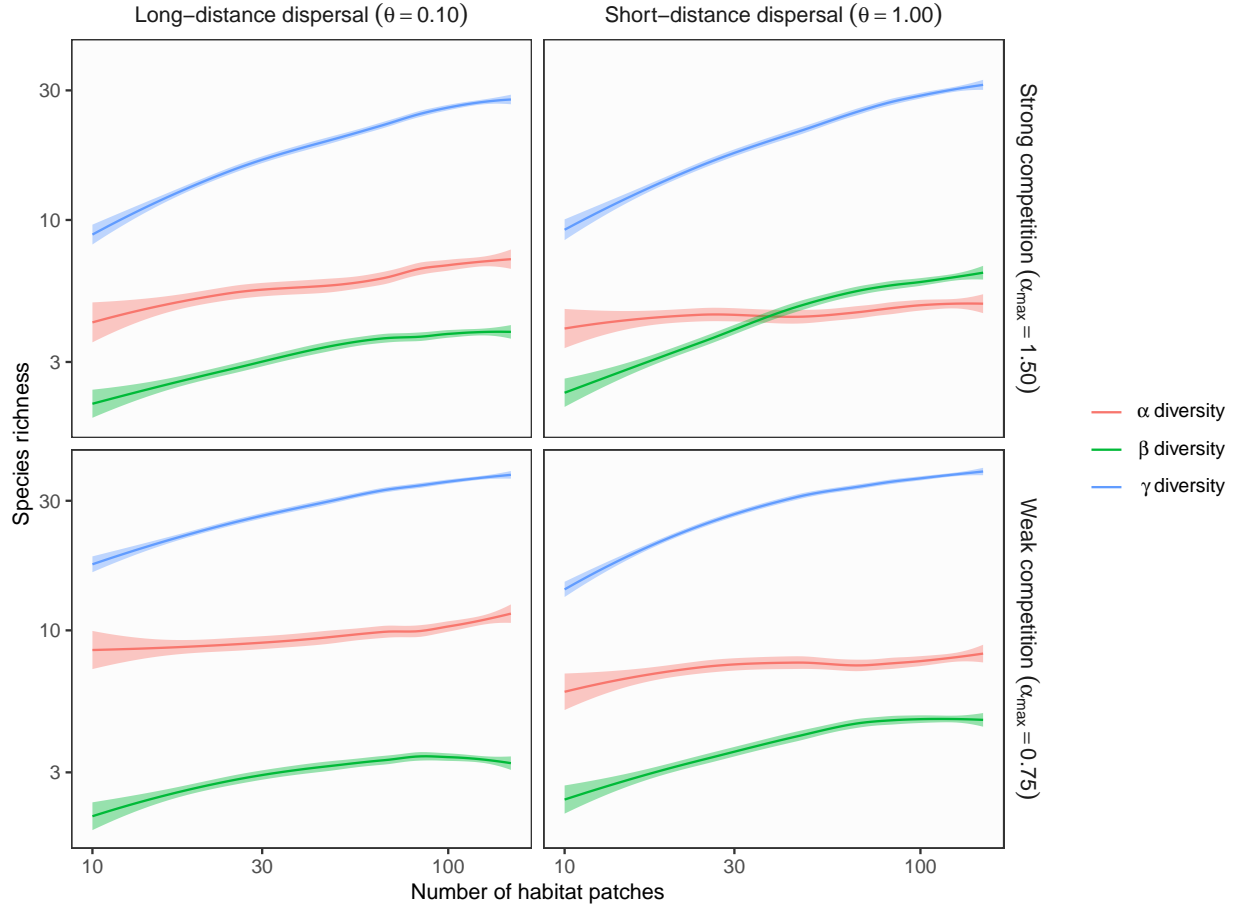


**Figure S7** Theoretical predictions for ecosystem size influences (the number of habitat patches) on  $\alpha$ ,  $\beta$ , and  $\gamma$  diversity in branching networks. In this simulation, environmental variation at headwaters ( $\sigma_h$ ) is less than local environmental noise ( $\sigma_l$ ). Lines and shades are loess curves fitted to simulated data and its 95% confidence intervals. Each panel represents different ecological scenarios under which metacommunity dynamics were simulated. Rows represent different competition strength. Competitive coefficients ( $\alpha_{ij}$ ) were varied randomly from 0 to 1.5 (top, strong competition) or 0.75 (bottom, weak competition). Columns represent different dispersal scenarios. Two dispersal parameters were chosen to simulate scenarios with long-distance (the rate parameter of an exponential dispersal kernel  $\theta = 0.10$ ) and short-distance dispersal ( $\theta = 1.0$ ). Other parameters are as follows: dispersal probability  $p_d = 0.01$ ; environmental variation at headwaters  $\sigma_h = 0.01$ ; local environmental noise  $\sigma_l = 1$ .

**Figure S8 Influence of ecosystem complexity ( $p_d = 0.1$ ,  $\sigma_h = 1$ ,  $\sigma_l = 0.01$ )**

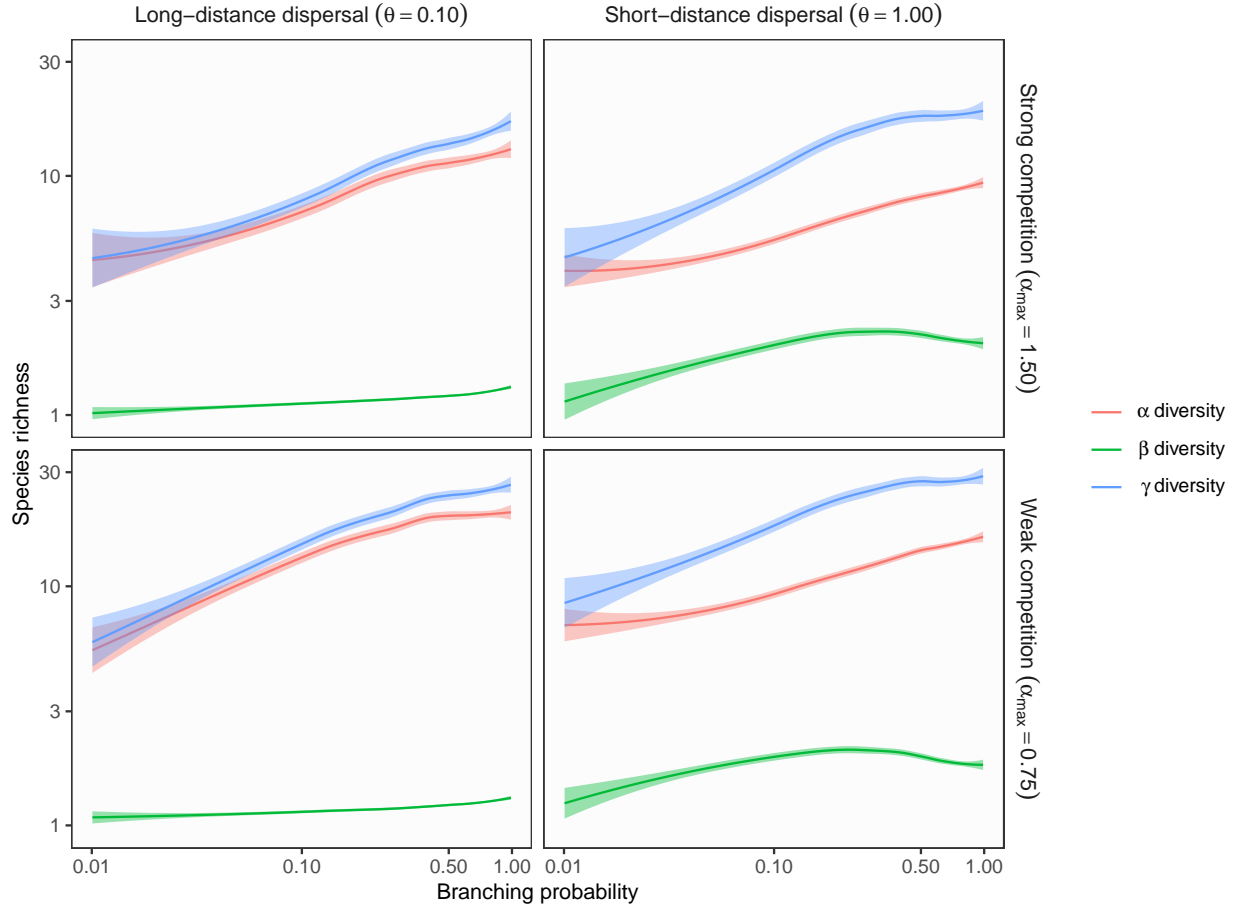


**Figure S8** Theoretical predictions for ecosystem complexity influences (branching probability) on  $\alpha$ ,  $\beta$ , and  $\gamma$  diversity in branching networks. In this simulation, environmental variation at headwaters ( $\sigma_h$ ) exceeds local environmental noise ( $\sigma_l$ ). Lines and shades are loess curves fitted to simulated data and its 95% confidence intervals. Each panel represents different ecological scenarios under which metacommunity dynamics were simulated. Rows represent different competition strength. Competitive coefficients ( $\alpha_{ij}$ ) were varied randomly from 0 to 1.5 (top, strong competition) or 0.75 (bottom, weak competition). Columns represent different dispersal scenarios. Two dispersal parameters were chosen to simulate scenarios with long-distance (the rate parameter of an exponential dispersal kernel  $\theta = 0.10$ ) and short-distance dispersal ( $\theta = 1.0$ ). Other parameters are as follows: dispersal probability  $p_d = 0.1$ ; environmental variation at headwaters  $\sigma_h = 1$ ; local environmental noise  $\sigma_l = 0.01$ .



**Figure S9 Influence of ecosystem complexity ( $p_d = 0.1$ ,  $\sigma_h = 1$ ,  $\sigma_l = 1$ )**

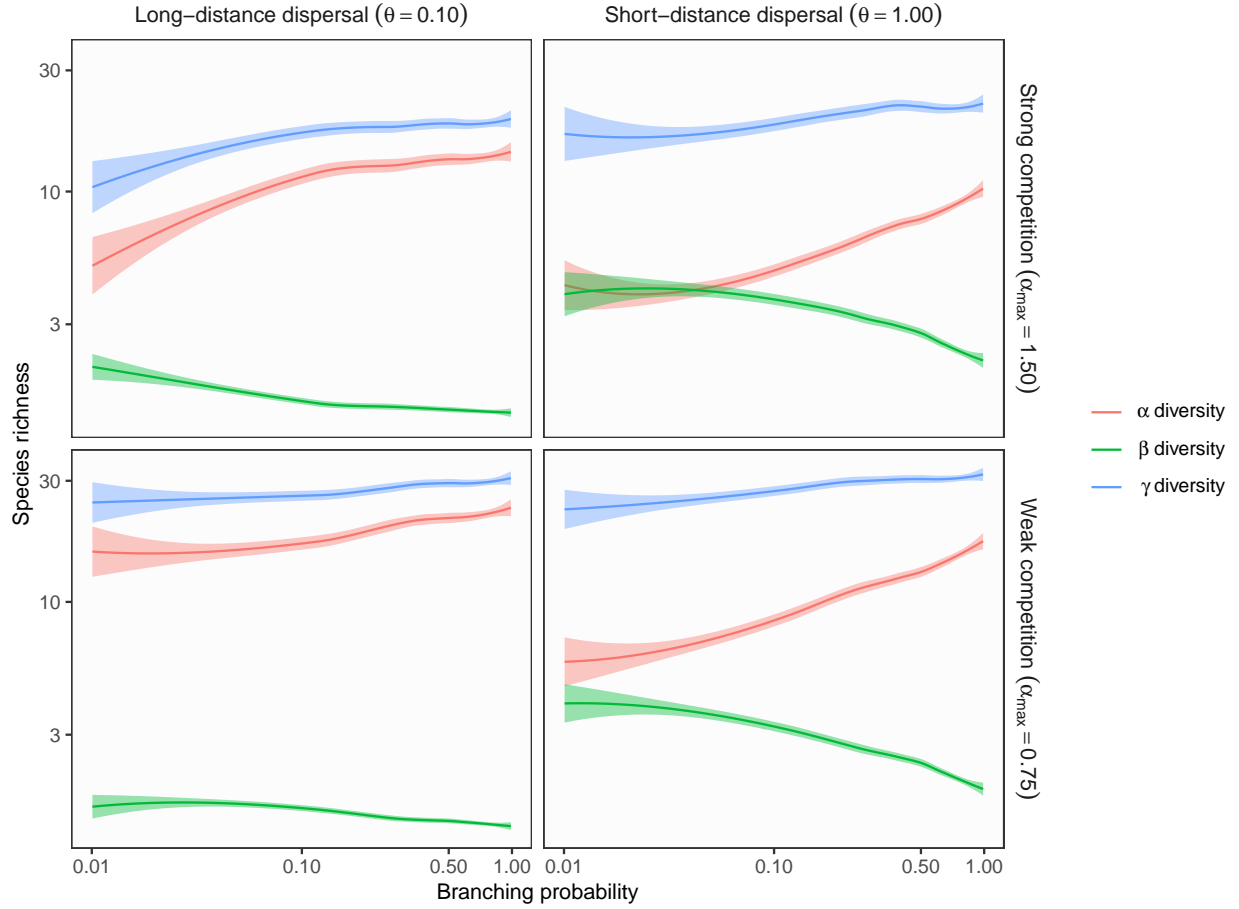


**Figure S9** Theoretical predictions for ecosystem complexity influences (branching probability) on  $\alpha$ ,  $\beta$ , and  $\gamma$  diversity in branching networks. In this simulation, environmental variation at headwaters ( $\sigma_h$ ) is equal to local environmental noise ( $\sigma_l$ ). Lines and shades are loess curves fitted to simulated data and its 95% confidence intervals. Each panel represents different ecological scenarios under which metacommunity dynamics were simulated. Rows represent different competition strength. Competitive coefficients ( $\alpha_{ij}$ ) were varied randomly from 0 to 1.5 (top, strong competition) or 0.75 (bottom, weak competition). Columns represent different dispersal scenarios. Two dispersal parameters were chosen to simulate scenarios with long-distance (the rate parameter of an exponential dispersal kernel  $\theta = 0.10$ ) and short-distance dispersal ( $\theta = 1.0$ ). Other parameters are as follows: dispersal probability  $p_d = 0.1$ ; environmental variation at headwaters  $\sigma_h = 1$ ; local environmental noise  $\sigma_l = 1$ .

**Figure S10** Influence of ecosystem complexity ( $p_d = 0.1$ ,  $\sigma_h = 0.01$ ,  $\sigma_l = 0.01$ )

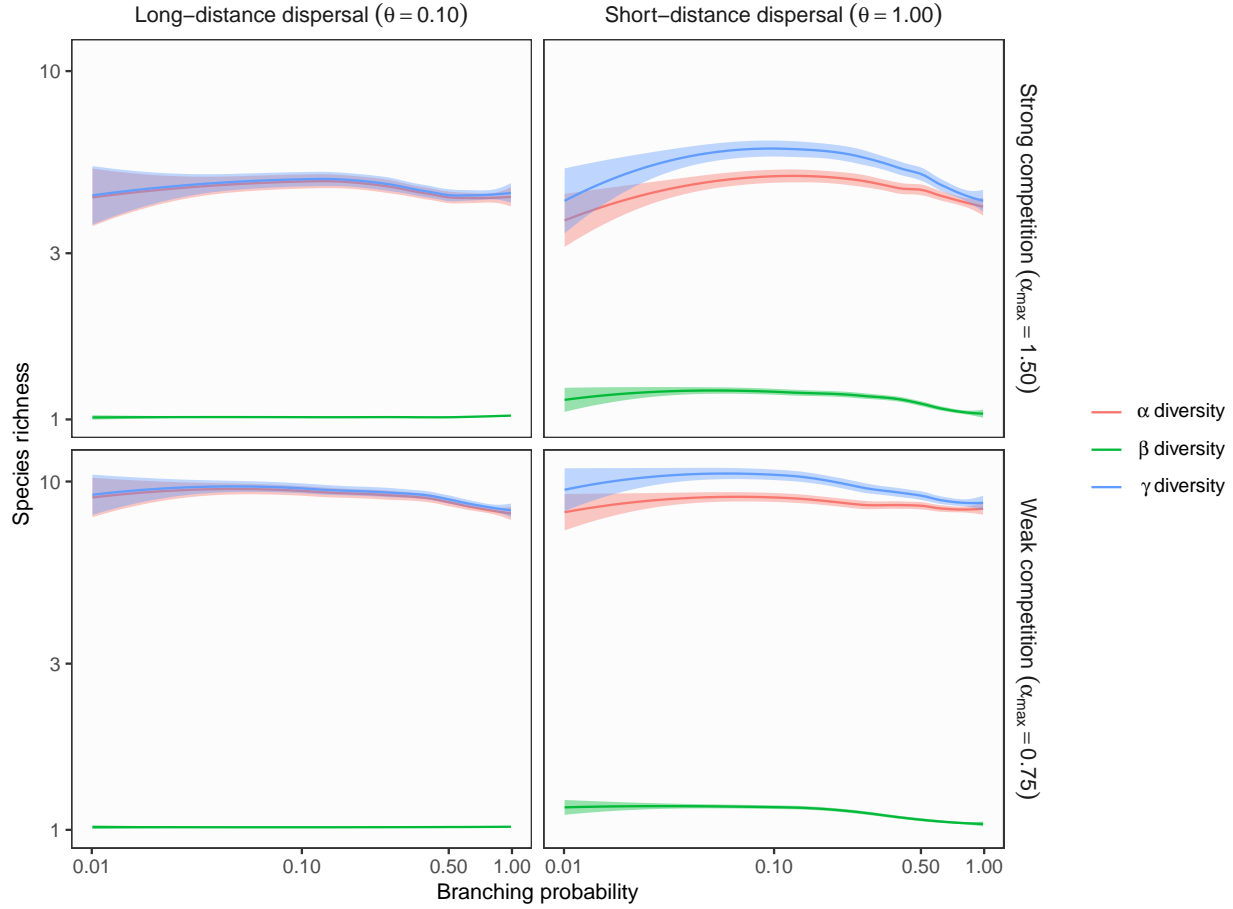


**Figure S10** Theoretical predictions for ecosystem complexity influences (branching probability) on  $\alpha$ ,  $\beta$ , and  $\gamma$  diversity in branching networks. In this simulation, environmental variation at headwaters ( $\sigma_h$ ) is equal to local environmental noise ( $\sigma_l$ ). Lines and shades are loess curves fitted to simulated data and its 95% confidence intervals. Each panel represents different ecological scenarios under which metacommunity dynamics were simulated. Rows represent different competition strength. Competitive coefficients ( $\alpha_{ij}$ ) were varied randomly from 0 to 1.5 (top, strong competition) or 0.75 (bottom, weak competition). Columns represent different dispersal scenarios. Two dispersal parameters were chosen to simulate scenarios with long-distance (the rate parameter of an exponential dispersal kernel  $\theta = 0.10$ ) and short-distance dispersal ( $\theta = 1.0$ ). Other parameters are as follows: dispersal probability  $p_d = 0.1$ ; environmental variation at headwaters  $\sigma_h = 0.01$ ; local environmental noise  $\sigma_l = 0.01$ .

**Figure S11** Influence of ecosystem complexity ( $p_d = 0.1$ ,  $\sigma_h = 0.01$ ,  $\sigma_l = 1$ )

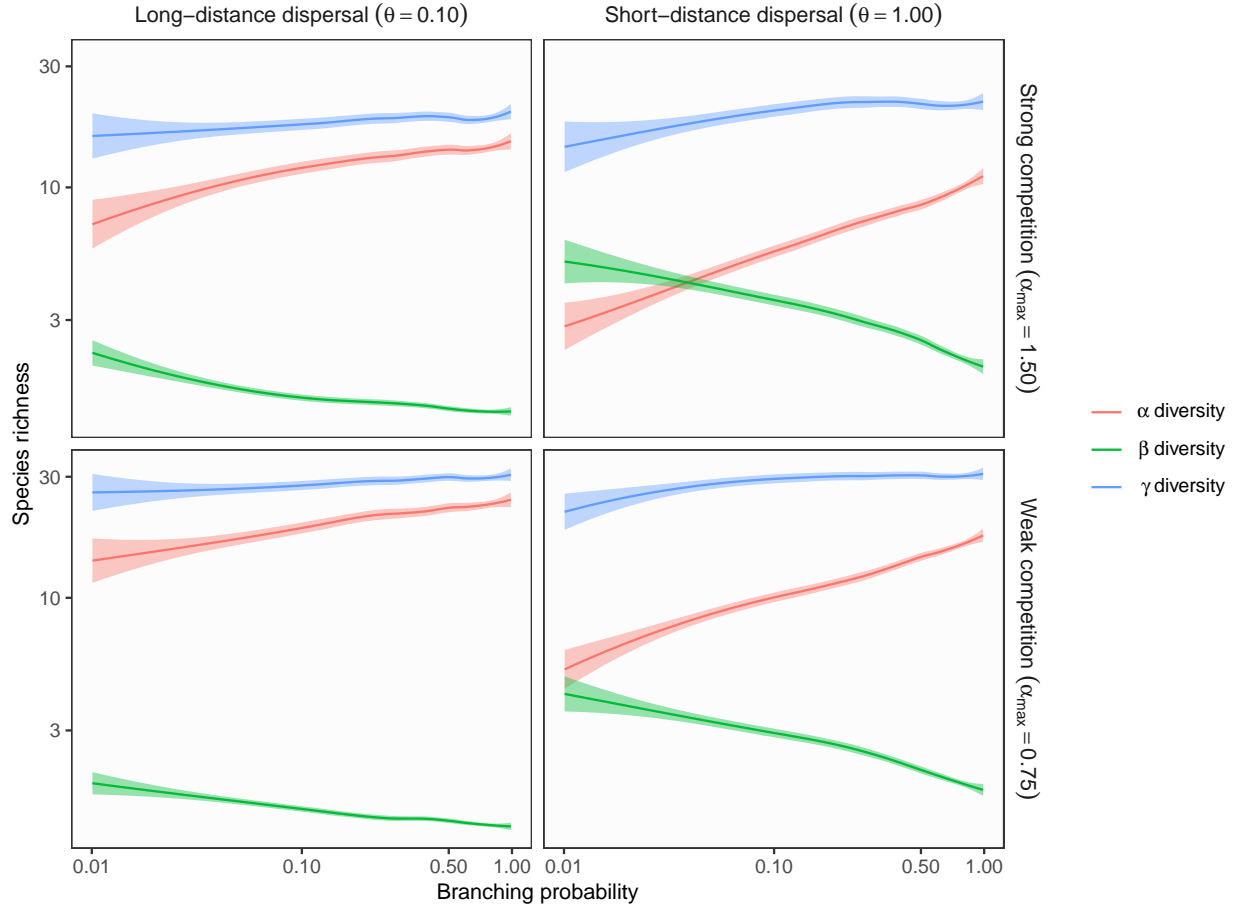


**Figure S11** Theoretical predictions for ecosystem complexity influences (branching probability) on  $\alpha$ ,  $\beta$ , and  $\gamma$  diversity in branching networks. In this simulation, environmental variation at headwaters ( $\sigma_h$ ) is less than local environmental noise ( $\sigma_l$ ). Lines and shades are loess curves fitted to simulated data and its 95% confidence intervals. Each panel represents different ecological scenarios under which metacommunity dynamics were simulated. Rows represent different competition strength. Competitive coefficients ( $\alpha_{ij}$ ) were varied randomly from 0 to 1.5 (top, strong competition) or 0.75 (bottom, weak competition). Columns represent different dispersal scenarios. Two dispersal parameters were chosen to simulate scenarios with long-distance (the rate parameter of an exponential dispersal kernel  $\theta = 0.10$ ) and short-distance dispersal ( $\theta = 1.0$ ). Other parameters are as follows: dispersal probability  $p_d = 0.1$ ; environmental variation at headwaters  $\sigma_h = 0.01$ ; local environmental noise  $\sigma_l = 1$ .

**Figure S12** Influence of ecosystem complexity ( $p_d = 0.01$ ,  $\sigma_h = 1$ ,  $\sigma_l = 1$ )

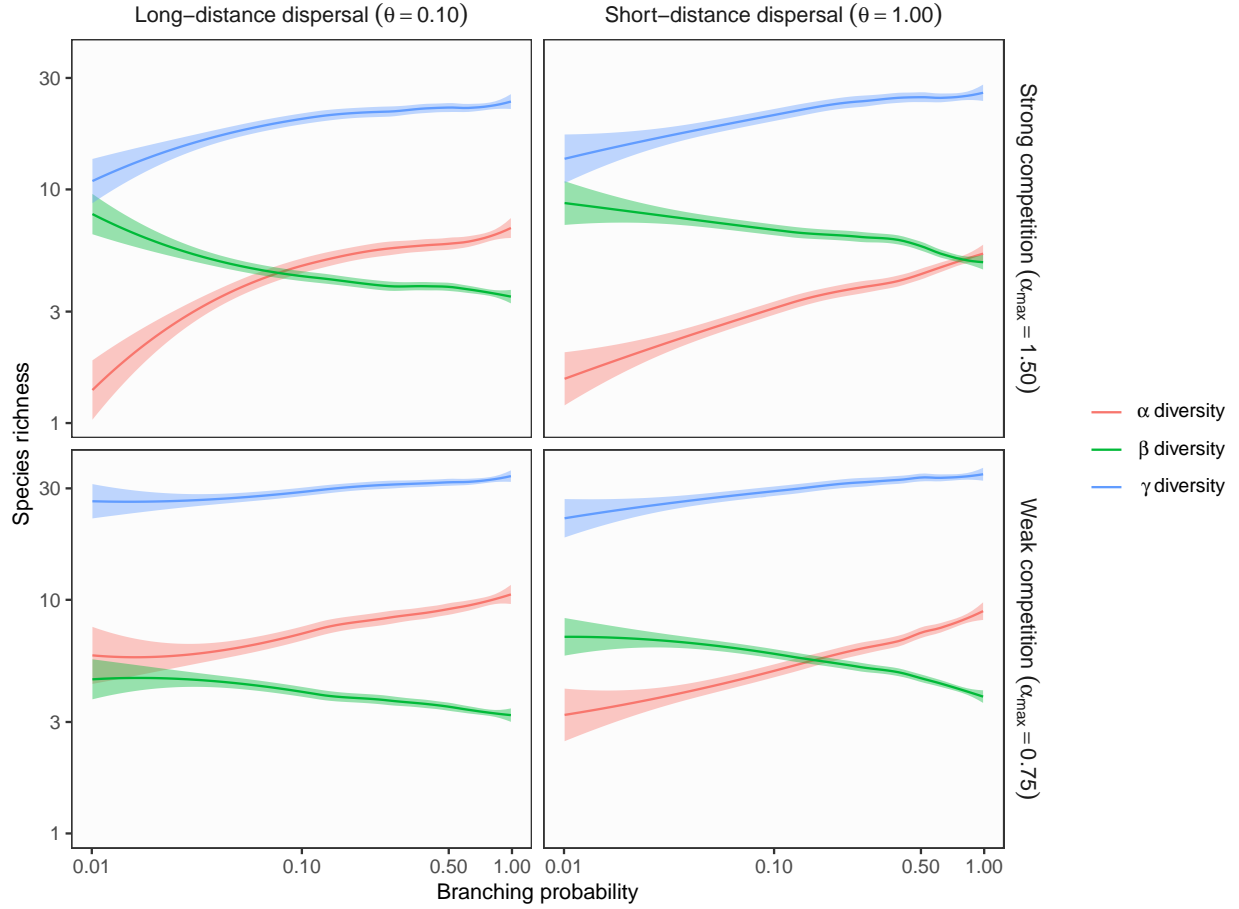


**Figure S12** Theoretical predictions for ecosystem complexity influences (branching probability) on  $\alpha$ ,  $\beta$ , and  $\gamma$  diversity in branching networks. In this simulation, environmental variation at headwaters ( $\sigma_h$ ) is equal to local environmental noise ( $\sigma_l$ ). Lines and shades are loess curves fitted to simulated data and its 95% confidence intervals. Each panel represents different ecological scenarios under which metacommunity dynamics were simulated. Rows represent different competition strength. Competitive coefficients ( $\alpha_{ij}$ ) were varied randomly from 0 to 1.5 (top, strong competition) or 0.75 (bottom, weak competition). Columns represent different dispersal scenarios. Two dispersal parameters were chosen to simulate scenarios with long-distance (the rate parameter of an exponential dispersal kernel  $\theta = 0.10$ ) and short-distance dispersal ( $\theta = 1.0$ ). Other parameters are as follows: dispersal probability  $p_d = 0.01$ ; environmental variation at headwaters  $\sigma_h = 1$ ; local environmental noise  $\sigma_l = 1$ .

**Figure S13 Influence of ecosystem complexity** ( $p_d = 0.01$ ,  $\sigma_h = 0.01$ ,  $\sigma_l = 0.01$ )

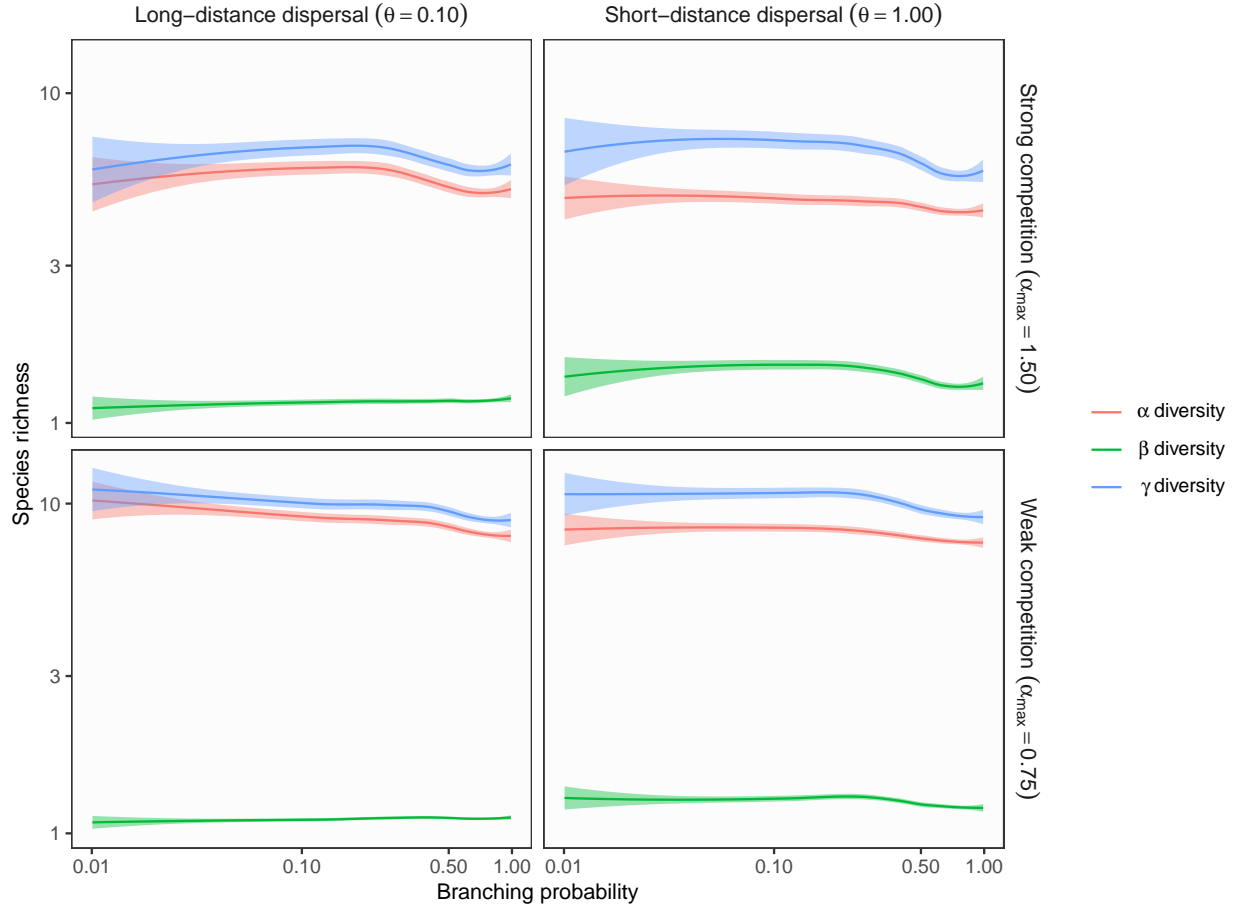


**Figure S13** Theoretical predictions for ecosystem complexity influences (branching probability) on  $\alpha$ ,  $\beta$ , and  $\gamma$  diversity in branching networks. In this simulation, environmental variation at headwaters ( $\sigma_h$ ) is equal to local environmental noise ( $\sigma_l$ ). Lines and shades are loess curves fitted to simulated data and its 95% confidence intervals. Each panel represents different ecological scenarios under which metacommunity dynamics were simulated. Rows represent different competition strength. Competitive coefficients ( $\alpha_{ij}$ ) were varied randomly from 0 to 1.5 (top, strong competition) or 0.75 (bottom, weak competition). Columns represent different dispersal scenarios. Two dispersal parameters were chosen to simulate scenarios with long-distance (the rate parameter of an exponential dispersal kernel  $\theta = 0.10$ ) and short-distance dispersal ( $\theta = 1.0$ ). Other parameters are as follows: dispersal probability  $p_d = 0.01$ ; environmental variation at headwaters  $\sigma_h = 0.01$ ; local environmental noise  $\sigma_l = 0.01$ .

**Figure S14** Influence of ecosystem complexity ( $p_d = 0.01$ ,  $\sigma_h = 0.01$ ,  $\sigma_l = 1$ )

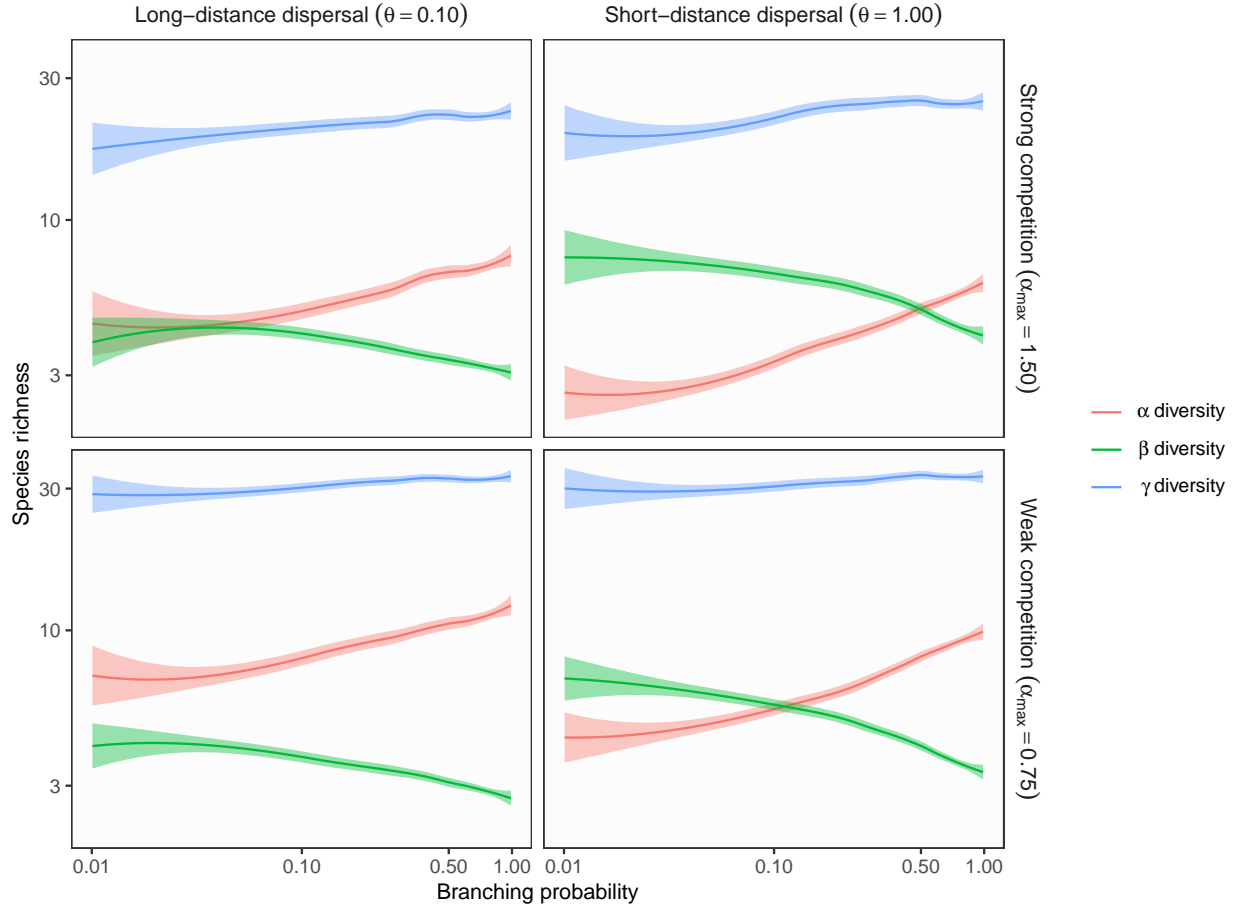


**Figure S14** Theoretical predictions for ecosystem complexity influences (branching probability) on  $\alpha$ ,  $\beta$ , and  $\gamma$  diversity in branching networks. In this simulation, environmental variation at headwaters ( $\sigma_h$ ) is less than local environmental noise ( $\sigma_l$ ). Lines and shades are loess curves fitted to simulated data and its 95% confidence intervals. Each panel represents different ecological scenarios under which metacommunity dynamics were simulated. Rows represent different competition strength. Competitive coefficients ( $\alpha_{ij}$ ) were varied randomly from 0 to 1.5 (top, strong competition) or 0.75 (bottom, weak competition). Columns represent different dispersal scenarios. Two dispersal parameters were chosen to simulate scenarios with long-distance (the rate parameter of an exponential dispersal kernel  $\theta = 0.10$ ) and short-distance dispersal ( $\theta = 1.0$ ). Other parameters are as follows: dispersal probability  $p_d = 0.01$ ; environmental variation at headwaters  $\sigma_h = 0.01$ ; local environmental noise  $\sigma_l = 1$ .

## References

1. Fukushima, M., Kameyama, S., Kaneko, M., Nakao, K. & Ashley Steel, E. Modelling the effects of dams on freshwater fish distributions in Hokkaido, Japan. *Freshwater Biology* **52**, 1511–1524 (2007).
2. Comte, L. *et al.* RivFishTIME: A global database of fish time-series to study global change ecology in riverine systems. *Global Ecology and Biogeography* **30**, 38–50 (2021).
3. Terui, A. *et al.* Metapopulation stability in branching river networks. *Proceedings of the National Academy of Sciences* **115**, E5963–E5969 (2018).
4. Terui, A. & Miyazaki, Y. Three ecological factors influencing riverine fish diversity in the Shubuto River system, Japan: Habitat capacity, habitat heterogeneity and immigration. *Limnology* **17**, 143–149 (2016).